

A substructure inside spiral arms, and a mirror image across the Galactic Meridian

Jacques P. Vallée

National Research Council Canada, Herzberg Astronomy & Astrophysics,
postal address: 5071 West Saanich Road, Victoria, B.C., Canada V9E 2E7
emails: jacques.p.vallee@gmail.com jacques.vallee@nrc-cnrc.gc.ca

Keywords: Galaxy: disk - Galaxy: structure – Galaxy: fundamental parameters –
ISM: kinematics and dynamics – Galaxy: formation

Abstract

While the galactic density wave theory is over 50 years old and well known in science, whether it fits our own Milky Way disk has been difficult to say. Here we show a substructure inside the spiral arms. This substructure is reversing with respect to the Galactic Meridian (longitude zero), and crosscuts of the arms at negative longitudes appear as mirror images of crosscuts of the arms at positive longitudes. Four lanes are delineated: mid-arm (extended ^{12}CO gas at mid arm, HI atoms), in-between offset by about 100 pc (synchrotron, radio recombination lines), in between offset by about 200 pc (masers, colder dust), and inner edge (hotter dust seen in Mid-IR and Near-IR).

1. Introduction

Elsewhere, in nearby external disk galaxies, the search for offsets between chemical tracers of spiral arms has been positive in some spiral galaxies, yet negative in some other galaxies, while it is ambiguous in other spiral galaxies such as in the giant galaxy M51 with negative and positive results (Louie et al 2013).

What is it in the Milky Way galaxy? The search for a substructure inside spiral arms in our Milky Way galaxy has been difficult, as we cannot easily observe in the optical domain far inside the galactic disk nor can we go above the galactic disk. Here, we use the tangent to each spiral arm, found when scanning the galactic disk in galactic longitudes, using different chemical tracers in the radio and far infrared domains. When looking through the tangent of a spiral arm, a peak intensity in that tracer appears. This observing technique cannot be done by us in any other galaxy, although a similar study could in principle be done in edge-on spiral galaxies.

Most of the chemical tracers employed to get the tangents for spiral arms inside the Milky Way are detected at radio wavelengths, although not all. Published arm tangents are listed in Vallée (2014a – his statistical table 3 has 43 arm tangents from 10 different tracers) and in Vallée (2014b – his statistical table 1 has 63 arm tangents from 14 different tracers), while in Appendix A here the statistical table 3 has 88 arm tangents from 18 different tracers, using 125 individual observations listed in Tables 4 to 10. These papers discovered for the first time that the dust lane in the Milky Way’s spiral arms was offset from the extended gas in the middle of the arm, notably by a few degrees in longitude from the center of the arm where the extended CO gas is mostly located. This CO tracer is the low-excitation J=1-0, low temperature (near 10 K), low-angular resolution (near 9’), narrow line (near 2 km/s) at 115 GHz, integrated over a velocity range commensurate with a spiral arm, from the Columbia survey.

Very recently, we did some analysis on the average offset between the arm edge and the arm center in the Milky Way galaxy. The average offset from the hot dust lane to the CO gas in mid-arm was found near $340 \text{ pc} \pm 56 \text{ pc}$, when averaging over all spiral arms with an observed tangent from the Sun (Fig. 2 in Vallée 2014b). This is now well established (a 6 sigma result).

Also, the average offset from the methanol maser to the CO gas in mid-arm was found *separately* for the group of so-called ‘major’ arms (Crux, Scutum. Perseus – 444 pc) and for the group of so-called ‘minor’ arms (Sagittarius, Carina, Norma – 401 pc), giving a width ratio = 1.1 ± 0.2 , essentially unity within the errors (Fig.3 in Vallée 2014a), and thus contrary to the putative existence of alternating ‘major’ (wide) and ‘minor’ (narrow) arms in the Milky Way.

Any arm substructure could be useful when attempting to place galactic filaments (very long, very thin, infrared dark clouds) in spiral arms, either at the spiral arm middle (Zucker et al 2015 – their fig.2), or else at the inner edge of spiral arm (Wang et al 2015 – their Sect. 4 .2), or outside in the inter-arm region (Ragan et al 2014 – their fig 4).

2. Updated Analysis – across the Galactic Meridian

Here, we analyse the offset of the dust to the CO gas peak, but *separately* at negative longitudes and at positive longitudes from the Galactic Center (longitude 0°).

Table 1 shows that the arm tangents for hot dust are offset inward from the arm tangents for the ^{12}CO , thus closer to the direction of the Galactic Center. Here the average offset between the red lane (dust) and the blue lane (mid arm, ^{12}CO) is about 315 pc, inside the solar orbit around the Galactic Center.

Figure 1 illustrates graphically this point. Galactic quadrants I corresponds to positive longitude l from 0 to 90 degrees, quadrant II to longitude l from 90 to 180, quadrant III from 180 to 270 degrees, and quadrant IV from 270 to 360 degrees (equivalently, from -90 to 0 degrees).

Although in Table 1 and Figure 1 some arms in quadrant IV appear to have a counterpart in quadrant I, these arms are not physically linked; the ^{12}CO gas in Crux-Centaurus arm at -51° is not linked to the ^{12}CO gas in the Sagittarius arm at $+51^\circ$; the hot dust in the Norma arm at -28° is not linked to the hot dust in the Scutum arm at $+29^\circ$.

A map of the Milky Way disk shows that the Crux-Centaurus arm is continuously linked to the Scutum arm, while the Carina arm is continuously linked to the Sagittarius arm, owing to a spiral pitch angle (a deviation from a circle) of about -13° (Vallée, 2015 – his fig.1).

3. New analysis – a mirror image across the Galactic Meridian

Here, we look for the presence of further lanes, in between the red (dust at arm's inner edge) lane and the blue (^{12}CO 1-0 gas at arm's middle), using an enlarged catalog of arm tangents (Appendix A, with 88 arm tangents from 18 different arm tracers).

The 4-arm structure in the Milky Way may encompass some substructures inside each spiral arm. We define here a 'substructure' when each different tracer is seen the same general arm at its own distance between the dust lane and the ^{12}CO 1-0 lane, but reversing on the other side of the Galactic Meridian (mirror image).

Table 2 shows the offset between two tangents, that of the ^{12}CO tracer direction as seen from the Sun and that of a specific arm tracer (molecule, atom, electron, excited gas, hot and cold dust). The angular offset is converted to a linear separation through its known distance from the Sun.

Figure 2 shows the mean arm crosscut, showing the offset for each tracer from the mid arm. They are averaged separately for the arms left of the Galactic

Meridian (quadrant IV) in Fig.2a, and right of the Galactic Meridian (quadrant I) in Fig.2b.

A blue lane encompasses the mid arm (including ^{12}CO). A red lane encompasses the arm's inner edge (including the hot dust). In between, we observe a 'substructure', namely one sees a green lane (near 100 pc, including relativistic synchrotron electrons, and radio recombination lines), and an orange lane (near 200 pc, including FIR [CII] and [NII] lines, radio masers, and colder dust at Extreme InfraRed).

At first glance, these two quadrants are mirror images – each lane (blue, green, orange, or red) is located at about the same place in linear separation. The mean arm width is about the same, with the red dust at 378 pc (left) and 340 pc (right), giving a ratio of 1.1 ± 0.3 , thus nearly equal within the errors.

4. Arm width with galactocentric distance

Finally, we reassess the possible enlargement with galactocentric distance of the arm half-width (offset between the red lane and the blue lane).

From the Notes in Table 1, using offsets from hot dust to ^{12}CO 1-0, one has a mean arm half-width for the Sagittarius and Scutum arms of 280 ± 69 pc in galactic quadrant I at a mean galactic distance of 4.5 kpc, which is smaller than the mean arm half-width for the continuation of these two arms into the other galactic quadrant IV (Carina and Crux-Centaurus) of 305 ± 44 pc at a mean galactic radius of 5.5 kpc, giving a ratio of 1.1 ± 0.3 , for a mean galactocentric distance ratio of 1.25 (see bottom of Table 1).

From Table 2, using offsets from cold dust (EIR - $870\mu\text{m}$) versus ^{12}CO 1-0, one has a mean arm half-width for the Sagittarius and Scutum arms of 136 ± 37 pc in galactic quadrant I at a mean galactic distance of 4.5 kpc, which is smaller than the mean arm half-width for the continuation of these two arms into the other galactic quadrant IV (Carina and Crux-Centaurus) of 225 ± 27 pc at a mean galactic radius of 5.5 kpc, giving a ratio of 1.6 ± 0.5 , for a mean galactocentric distance ratio of 1.25.

A statistical mean of these two observed arm ratios gives a rough value of 1.35 at a distance ratio of 1.25.

Table 1 – Arm tangents to two arm tracers (hot dust; extended ^{12}CO gas), in galactic longitude, using a Sun to Galactic Center distance of 8.0 kiloparsecs

	^{12}CO tangent at gal. longit. (degrees)	dust tangent at gal. longit. (degrees)	angular difference (degrees)	linear difference (parsecs)	Note
Carina arm	-79	-75	4	350 (at 5kpc)	1
Crux-Cent. Arm	-51	-48.5	2.5	260 (at 6kpc)	1
Norma arm	-31	-28	3	370 (at 7kpc)	
Perseus-start arm	-23.5	-21	2.5	350 (at 8kpc)	
Scutum arm	+33	+29	4	350 (at 5kpc)	2
Sagittarius arm	+51	+48	3	210 (at 4 kpc)	2
Mean and s.d.m.	-	-	3.2 ± 0.3	315 ± 26	

Note 1: the mean offset for Carina and Crux-Centaurus is 305 ± 44 pc at a mean solar distance of 5.5 kpc (mean galactocentric distance of 7.5 kpc).

Note 2: the mean offset for Scutum and Sagittarius is 280 ± 69 pc at a mean solar distance of 4.5 kpc (mean galactocentric distance of 6 kpc).

Table 2 – Separation (offset) from the mid arm (^{12}CO)

1	2	3	4	5	6	7	8	9	10	11
	^{12}CO mol. pc	ther. el. pc	HI atom pc	relat. el. pc	reco. el. pc	EIR dust pc	FIR [CII] pc	radio maser pc	MIR dust pc	NIR dust pc
Carina arm	0	148	22	-	262	253	497	-	322	-
Crux-Cent. Arm	0	-52	42	52	178	198	-52	-	157	-
Norma arm	0	-49	-37	-49	110	147	-	244	73	449
Perseus-start arm	0	-	0	307	14	140	167	140	446	307
Mean	0	16	07	103	141	184	204	192	250	378
S.d.m .	-	± 66	± 17	± 105	± 52	± 26	± 159	± 51	± 83	± 70
Scutum arm	0	78	166	78	183	174	253	384	602	340
Sagittarius arm	0	105	-7	175	91	98	35	35	-	-
Mean	0	91	80	126	137	136	144	210	602	340
S.d.m .	-	± 31	± 86	± 48	± 46	± 27	± 108	± 173	-	± 70

Note. Column 1 is the spiral arm name, Columns 2 to 11 have the offset, from the ^{12}CO tangent, of a specific arm tracer tangent, namely the thermal electron, the HI atom, the relativistic synchrotron electron, HII recombining electrons (radio recombination line at 1.4 GHz), the Extreme InfraRed dust (870 microns), the Far InfraRed [CI] and [NII] lines, the radio masers (mostly methanol), the Mid InfraRed dust (60 microns), and the Near InfraRed dust (2.4 microns). The S.d.m. is the standard deviation of the mean.

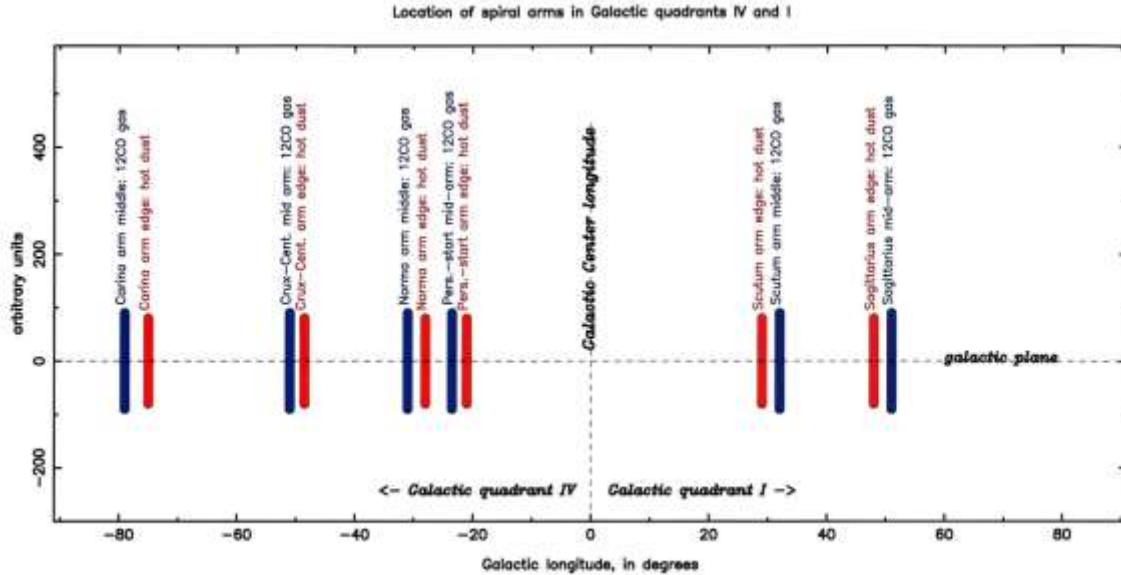


Figure 1. Location in galactic longitude (x-axis) of several spiral arms, indicating the tangent to each spiral arm as seen from the Sun, using two arm tracers (^{12}CO J=1-0 extended gas, hot dust). An evident reversal of these two tracers is observed as one goes across the Galactic Meridian (located at galactic longitude zero). Vertical axis is arbitrary. In each arm, it can be seen that the red lane (hot dust) is always closer to the Galactic Meridian (located at longitude $l=0^\circ$). Thus the dust lane (red) is to the right of the blue lane (mid arm, ^{12}CO) when at a negative galactic longitude (quadrant IV), and is reversing to be at the left of the mid arm when at positive galactic longitude (quadrant I).

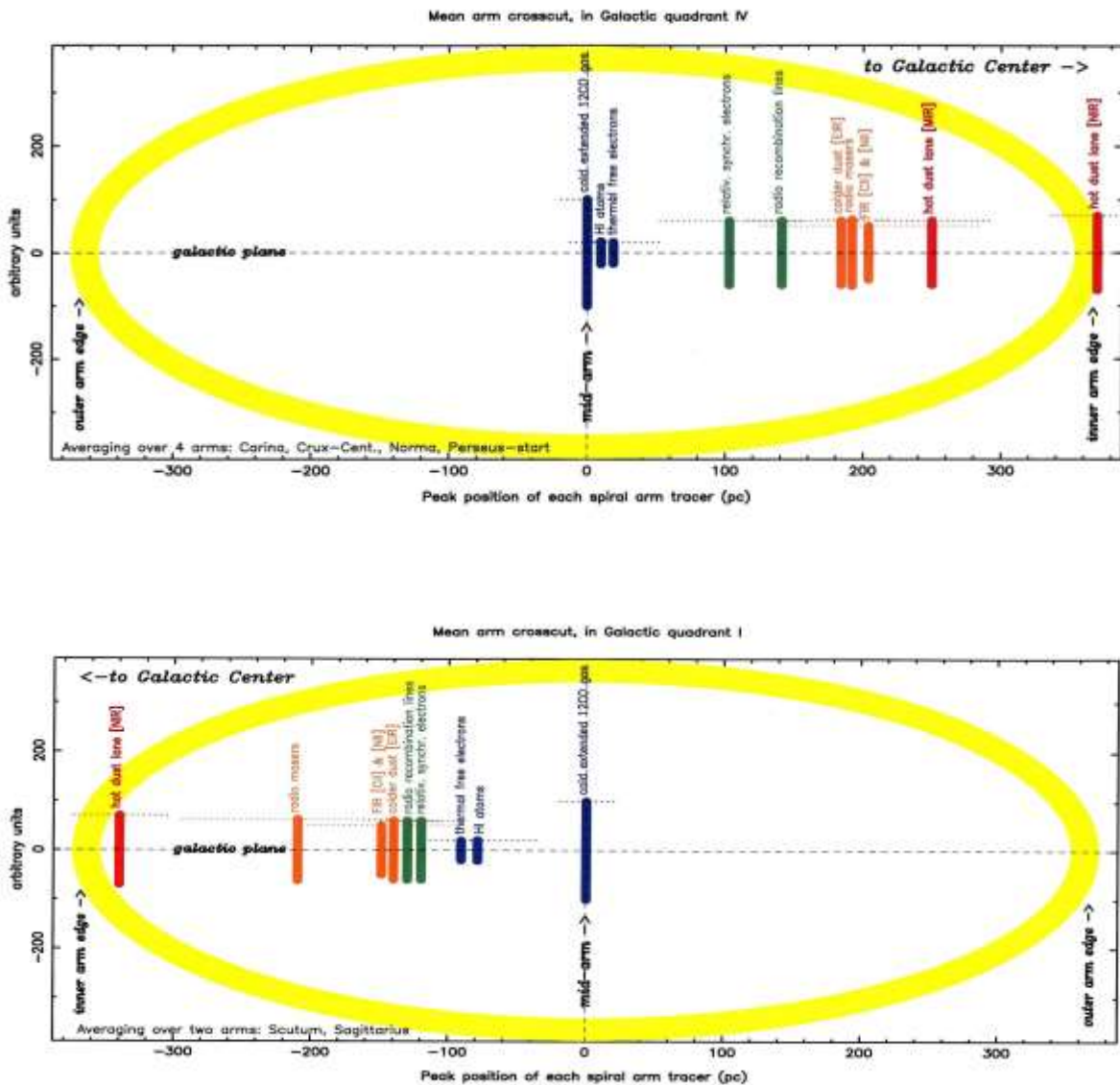


Figure 2. Location of the tangents for several arm tracers, each tracer being averaged over several spiral arms in quadrant IV (Fig.2a) and in Quadrant I (fig.2b). Galactic Center direction (arrow at top) is indicated in each quadrant. These figures are almost mirror images. Blocks of tracers, having similar distances, are shown: hot dust at the inner arm edge (red), mid arm extended ^{12}CO J=1-0 gas (blue), and in between blocks near 100pc (green) and near 200pc (orange) as measured from the mid arm. Tangential arm offsets are translated in linear offsets, using the known tangential arm distance (from Table 1). The overall yellow ellipse indicates a very rough limit for the extent of the arm stars.

5. Interpretation and Comparison

Not many theories of spiral arms predict a reversal of dust position across the Galactic Meridian, nor of additional substructures inside a spiral arm. A recent review of different theories to produce spiral arms is given by Dobbs and Baba (2014). Here we focus our interpretation using predictions from the density wave theory.

a- Reversal of the inner arm edge with the Galactic Meridian (Section 2):

Density wave theory (Lin & Shu 1964; Lin et al 1969) predicts that the interarm gas, in a circular orbit around the Galactic Center, will overtake a slower moving spiral pattern, and be shocked at the entrance (leading to a hot dust lane), thus the hot dust lane would face inward toward the Galactic Center (below a galactic radius called co-rotation, at about 9 kpc in the Milky Way disk). In the density wave theory, the dust lane corresponds to the predicted location of a shock lane.

In our Milky Way disk galaxy, radio and infrared observations of the arm tangents showed objectively that a reversal between hot dust and mid arm do appear (Figure 1, Table 1), and that a 4-arm structure is needed.

b- Substructures within an arm (Section 3):

Past the shock lane, density wave theory predicts a decrease of gas density and gas temperature, as the orbiting gas penetrates deeper toward the colder arm middle, leading to the prediction of some substructures (regions between the inner arm edge's dust lane and the mid-arm lane in the center). In the density wave theory, the middle of the arm corresponds to the lane with a potential maximum.

In the density wave model of Roberts (1975 – his Fig. 2), along a typical gas streamline around the Galactic Center, a shock (gas density of 5 units) precedes the potential minimum (gas density near 2.5 units), and the orbit brings it to the zero potential (gas density near 1.25 units) and onward to the potential maximum (mid arm; gas density near 0.7 unit), with the gas density being relatively stable afterwards.

The substructure in an arm, predicted by the density wave as a function of the orbit, is theoretical and usually made for a 2-arm spiral model. They should not be expected to be the same, but they should still be close, to the 4 observed substructures in a typical Milky Way's arm.

In the Milky Way disk galaxy, the observational existence of similar gas compositions (substructures) at different offsets from the dust lanes, appears here as some kind of mirror images across the Galactic Meridian (Figure 2, Table 2).

c- Enlargement of an arm width with distance (Section 4):

Density wave theory predicts a weak opening of a spiral arm as a function of galactic distance. In the density wave theory, a small opening of each spiral arm is predicted as a function of increasing radial distance from the Galactic Center.

A 2-arm theoretical map of the Carina-Sagittarius arm by Lin et al (1969 – their fig. 4), drawn for a Sun to Galactic Center distance of 10 kpc and an arm pitch angle near -6° , shows an arm width of 1.9 kpc at the arm tangent to Carina at a galactocentric radius of 8.3 kpc, and an arm width of 1.1 kpc at the arm tangent to Sagittarius at a galactocentric radius of 7.3 kpc, thus giving an arm ratio of 1.7 at a galactic radius ratio of 1.14.

The same theoretical map of the Crux-Centaurus-Scutum arm by Lin et al (1969 – their fig. 4) shows an arm width of 1.2 kpc at the arm tangent to Crux-Centaurus at a galactocentric radius of 5.4 kpc, and an arm width of 0.85 kpc at the arm tangent to Scutum at a galactocentric radius of 4.8kpc, thus giving an arm ratio of 1.4 at a galactic radius ratio of 1.12.

A statistical mean of these two theoretical arm ratios gives a rough value of 1.55 at a distance ratio of 1.13.

6. Conclusion

Based on observed arm tangents, we presented statistical results and graphic figures about substructures in the spiral arms in the Milky Way. Substructures (parallel lanes) are observed between the dust lane and the middle of the arm (extended ^{12}CO 1-0 gas lane) – see Figure 1 and Table 1.

Furthermore, when comparing a graph of an average of the offsets within spiral arms at negative galactic longitudes (Fig. 2a) with a graph of the offsets within spiral arms at positive galactic longitudes (Figure 2b), we obtain a rough mirror image.

These data tend to support several predictions from the density wave theory, as applied to our Milky Way galaxy. With increasing galactic radius, we statistically deduce a weak enlargement of the offset between dust lane and mid arm.

Appendix A

Appendix A is an updated compilation of arm tangents, as statistically averaged for each tracer (Table 3), and individually listed for each tracer (Tables 4 to 10). Earlier such catalogues were given in Vallée (2014a; 2014b).

Acknowledgements.

The figure production made use of the PGPLOT software at the NRC Canada in Victoria, BC. I thank a referee for clarification.

References

- Alvarez, H. May, J., Bronfman, L., "The rotation of the Galaxy within the solar circle", 1990, *Astrophys. J.*, v348, p495-502.
- Anderson, L.D., Bania, T.M., Balser, D.S., Cunningham, V., Wenger, T.V., Johnstone, B.M., Armentrout, W.P., "The WISE catalog of galactic HII regions", 2014, *ApJ SS*, v212, a1, p1-18.
- Bajaja, E., Arnal, E., Larrarte, J, and 3 others, "A high sensitivity HI survey of the sky at $\text{dec} < -25^\circ$. Final data release", 2005, *A&A*, v440, p767-773.
- Benjamin, R.A., Churchwell, E., Babler, B.L., Bania, T.M., Clemens, D.P., Cohen, M., and 14 others. "GLIMPSE. I. An SIRTf Legacy Project to map the inner Galaxy", 2003, *Publ. Astron Soc Pacific*, v115, p953-964.
- Benjamin, R.A., "The spiral structure of the Galaxy: something old, something new", 2008, *ASP Conf. Ser.*, edited by H.Beuther, H.Linz, Th.Henning, v387, p375-380.
- Beuermann, K., Kanbach, G., Berkhuijsen, E.M., "Radio structure of the Galaxy – Thick disk and thin disk at 408 MHz", 1985, *A&A*, v153, p17-34.
- Beuther, H., Tackenberg, J., Linz, H., Henning, Th., Schuller, F., Wyrowski, F, Schilke, P., Menten, K., Robitaille, T.P., Wlamsley, C.M., Bronfman, L., Motte, F., Nguyen-Luong, Q., Bontemps, S., "Galactic structure based on the Atlasgal 870 μm survey", 2012, *ApJ*, v747, a43, p1-8.
- Bloemen, J.B., Deul, E.R., Thaddeus, P., "Decomposition of the FIR Milky Way observed by IRAS", 1990, *A&A*, v233, p437-455.
- Bronfman, L., "Molecular clouds and young massive stars in the Galactic disk", 1992, *Astrophys Space Sci Lib.*, v180, p131-154.
- Bronfman, L. "Massive star formation in the southern Milky Way", 2008, *Ap Sp Sci.*, v313, p81-85.
- Bronfman, L., Alvarez, H., Cohen, R.S., Thaddeus, P., "A deep CO survey of molecular clouds in the southern Milky Way", 1989, *ApJ Suppl Ser.*, v71, p481-548.
- Bronfman, L., Casassus, S., May, J., Nyman, L.-A., "The radial distribution of OB star formation in the Galaxy", 2000a, *Astron. & Astrophys.*, v358, p521-534.
- Bronfman, L., Cohen, R.S., Alvarez, H., May, J., Thaddeus, P., "A CO survey of the southern Milky Way: the mean radial distribution of molecular clouds within the solar circle", 1988, *ApJ*, v324, p248-266.
- Bronfman, L., May, J., Luna, A., "A CO survey of the southern Galaxy", 2000b, *ASP Confer. Ser.*, edited by J.Mangum & S.Radford, v217, p66-71.
- Caswell, J.L., Fuller, G.A., Green, J.A., Avison, A., Breen, S.L., Ellingsen, S.P., Gray, M.D., Pestalozzi, M.R., Quinn, L., Thompson, M.A., Voronkon, M.A., "The 6GHz methanol

multibeam maser catalogue – III. Galactic longitudes 330° to 345°”, 2011, MNRAS, v417, p1964-1995.

Chen, W., Gehrels, N., Diehl, R., Hartmann, D., “ On the spiral arm interpretation of Comptel ^{26}Al map features”, 1996, A&A Suppl., v120, p315.

Chiar, J.E., Kutner, M.L., Verter, F., Leous, J., “A comparison of CO (J=1-0) and CO (J=2-1) emission in the Milky Way molecular ring”, 1994, ApJ, v431, p658-673.

Cohen, R.S., Cong, H., Dame, T.M., Thaddeus, P., “Molecular clouds and galactic spiral structure”, 1980, ApJ, v239, L53-L56.

Contreras, Y., Schuller, F., Urquhart, J.S., Csengeri, T., Wyrowski, F., Beuther, H., Bontemps, S., and 8 others, “ATLASGAL – compact source catalogue: $330^\circ <l < 21^\circ$ ”, 2013, A&A, v 549, A45, p1-15.

Csengeri, T., Urquhart, J.S., Schuller, F., Motte, F., Bontemps, S., Wyrowski, F., and 8 others, “The ATLASGAL survey: a catalog of dust condensations in the Galactic Plane”, 2014, A&A, v565, a75, p1-21.

Dame, T.M., Elmegreen, B.G., Cohen, R.S., Thaddeus, P., “The largest molecular cloud complexes in the first galactic quadrant”, 1986, ApJ, v305, p892-908.

Dame, T.M., Hartmann, D., Thaddeus, P., “The Milky Way in molecular clouds: a new complete CO survey”, 2001, ApJ., v547, p.792-813.

Dame, T.M., Thaddeus, P., “A new spiral arm of the Galaxy: the Far 3kpc arm”, 2008, ApJ, v683, L143-L146.

Dame, T.M., Thaddeus, P., “A molecular spiral arm in the far outer galaxy”, 2011, ApJL, v734, L24, p1-4.

Dobbs, C., Baba, J., “Dawes Review 4: Spiral structures in disc galaxies”, 2014, Publ. Astr. Soc. Australia, v31, a35, p1-40.

Downes, D., Wilson, T.L., Bieging, J., Wink, J., “ H110 α and H₂CO survey of galactic radio sources”, 1980, A&A Suppl., v40, p379-394.

Drimmel, R., “Evidence for a 2-armed spiral in the Milky Way”, 2000, A&A, v358, L13-L16.

Englmaier, P., Gerhard, O., “ Gas dynamics and large-scale morphology of the Milky Way galaxy “, 1999, MNRAS, v304, p512-534.

García, P., Bronfman, L., Nyman, L.-A., Dame, T.M., Luna, A., “ Giant molecular clouds and massive star formation in the southern Milky Way”, 2014, AstrophysJSuppl.Ser., v212, a2, p1-33.

Grabelsky, D.A., Cohen, R.S., Bronfman, L., Thaddeus, P., May, J., “ Molecular clouds in the Carina arm – largescale properties of molecular gas and comparison with HI”, 1987, Astrophysical journal, v315, p122-141.

Grabelsky, D.A., R.S. Cohen, L. Bronfman, P. Thaddeus, “ Molecular clouds in the Carina arm – the largest objects, associated regions of star formation, and the Carina arm in the Galaxy”, 1988, Astrophysical journal, v331, p181-196.

Green, J.A., Caswell, J.L., McClure-Griffiths, N.M., Avison, A., Breen, S.L., Burton, M.G., Ellingsen, S.P., Fuller, G.A., Gray, M.D., Pestalozzi, M., Thompson, M.A., Voronkov, M.A., “Major structures of the inner Galaxy delineated by 6.7GHz methanol masers”, 2011, ApJ, v733, a27, p1-17.

Green, J.A., Caswell, J.L., McClure-Griffiths, N.M., Avison, A., Breen, S.L., Burton, M.G., Ellingsen, S.P., Fuller, G.A., Gray, M.D., Pestalozzi, M., Thompson, M.A., Voronkov, M.A., “Tracing major structures of the inner Galaxy with 6.7GHz methanol masers”, 2012, EPJ Web of conferences, edited by C.Reylé, A.Robin, & M. Schultheis, v19, a06007, p1-3.

Hartmann, D., Burton, W., “Atlas of galactic neutral Hydrogen”, 1997, Cambridge Univ. Press, Cambridge, UK, p243.

Hayakawa, S., Matsumoto, T., Murakami, H., Uyama, K., Thomas, J.A., Yamagami, T., "Distribution of near infrared sources in the galactic disk", 1981, A&A, v100, p116.

Hou, L.G., Han, J.L., "The observed spiral structure of the Milky Way", 2014, A&A, v569, a125, p1-23.

Hou, L.G., Han, J.L., "Offset between stellar spiral arms and gas arms of the Milky Way", 2015, MNRAS, v. 454, p626-636.

Jackson, J.M., Rathborne, J.M., Shah, R.Y., Simon, R., Bania, T.M., Clemens, D.P., Chambers, E.T., Johnson, A.M., Dormody, M., Lavoie, R., "The Boston university five-college radioastronomy observatory Galactic ring survey", 2006, ApJ SS, v163, p.145-159.

Kalberla, P.M.W., Burton, W.B., Hartmann, D., Arnal, E.M., Bajaja, E., Morras, R., Poppel, W.G., "The Leiden/Argentine/Bonn (LAB) survey of galactic HI – Final data release of the combined LDS and IAR surveys with improved stray-radiation corrections", 2005, A&A, v440, p775-782.

Kretschmer, K., Diehl, R., Krause, M., Burkert, A., Fierlinger, K., Gerhard, O., Greiner, J., Wang, W., "Kinematics of massive star ejecta in the Milky Way as traced by ^{26}Al ", 2013, A&A, v559, a99, p1-11.

Lin, C.C., Shu, F.H., "On the spiral structure of disk galaxies", 1964, ApJ., v140, p646-655.

Lin, C.C., Yuan, C., Shu, F.H., "On the spiral structure of disk galaxies. III. Comparison with observations", 1969, ApJ, v155, p721-746.

Louie, M., Koda, J. Egusa, F., "Geometric offsets across spiral arms in M51: nature of gas and star formation tracers", 2013, ApJ, v763, a94, p1-11.

Nakanishi, H., Sofue, Y., "Three-dimensional distribution of the ISM in the Milky Way galaxy. III. The total neutral gas disk", 2016, Pub Astr Soc Japan, v68, a5, p 1-14.

Pandian, J.D., Goldsmith, P.E., "The Arecibo methanol maser galactic plane survey. II. Statistical and multiwavelength counterpart analysis", 2007, ApJ, v669, p435-445.

Ragan, S.E., Henning, Th., Tackenberg, J., Beuther, H., Johnston, K.G., Kainulainen, J., Linz, H., "Giant molecular filaments in the Milky Way", 2014, A & A, v568, a73, p1-22.

Reid, M.J., Menten, K.M., Brunthaler, A., Zheng, X.W., Dame, T.M., Xu, Y., Wu, Y., Zhang, B., and 8 others, "Trigonometric parallaxes of high mass star forming regions: the structure and kinematics of the Milky Way", 2014, ApJ, v783, a130, p1-14.

Roberts, W.W., "Theoretical aspects of galactic research", 1975, Vistas in Astron., v19, p91-109.

Russeil, D., "Star-forming complexes and the spiral structure of our Galaxy", 2003, A&A, v397, p133-146.

Russeil, D., Adami, C., Georgelin, Y.M., "Revised distances of Northern HII regions", 2007, A&A, v470, p161-171.

Sanders, D.B., Scoville, N.Z., Solomon, P.M., "Giant molecular clouds in the Galaxy. II. Characteristics of discrete features", 1985, ApJ, v289, p373-387.

Sanna, A., Reid, M.J., Menten, K.M., Dame, T.M., Zhang, B., Sato, M., Brunthaler, A., Moscadelli, L., Immer, K., "Trigonometric parallaxes to star-forming regions within 4 kpc of the Galactic Center", 2014, ApJ, v781, a108, p1-13.

Sato, M., Wu, Y.W., Immer, K., Zhang, B., Sanna, A., Reid, M.J., Dame, T.M., Brunthaler, A., Menten, K.M., "Trigonometric parallaxes of star forming regions in the Scutum spiral arms", 2014, ApJ, v793, a72, p1-15.

Skrutskie, M.F., Cutri, R.M., Stiening, R., Weinberg, M.D., Schneider, S., Carpenter, J.M., and 25 others, "The Two Micron All Sky Survey (2MASS)", 2006, AJ, v131, p1163-1183.

Solomon, P.M., Sanders, D.B., Rivolo, A.R., "The Massachusetts-Stony-Brook galactic plane CO survey: disk and spiral arm molecular cloud populations", 1985, ApJ, v292, L19-L24.

Stark, A.A., Lee, Y., “Giant molecular clouds are more concentrated toward spiral arms than smaller clouds”, 2006, ApJ, v641, L113-L116.

Steiman-Cameron, T.Y., Wolfire, M., Hollenbach, D., “COBE and the galactic interstellar medium: geometry of the spiral arms from FIR cooling lines”, 2010, ApJ, v722, p1460-1473.

Taylor, J.H., Cordes, J.M., “Pulsar distances and the galactic distribution of free electron”, 1993, ApJ, v411, p674-684.

Vallée, J.P., “The spiral arms of the Milky Way: the relative location of each different arm tracer, within a typical spiral arm width”, 2014a, Astron. J., v.148, A5, p.1-9.

Vallée, J.P., “Catalog of observed tangents to the spiral arms in the Milky Way Galaxy”, 2014b, Astrophys J Suppl Ser., v215, a1, p1-9.

Vallée, J.P., “Different studies of the global pitch angle of the Milky Way’s spiral arms”, 2015, MNRAS, v450, p4277-4284.

Vallée, J.P., “The start of the Sagittarius spiral arm (Sagittarius origin) and the start of the Norma spiral arm (Norma origin) – model-computed and observed arm tangents at galactic longitudes $-20^{\circ} < l < +23^{\circ}$ ”, 2016, Astron. J., v151, a55, p1-16.

Velusamy, T., Langer, W.D., Goldsmith, P.F., Pineda, J.L., “Internal structure of spiral arms traced with [CII]: unraveling the WIM, HI, and molecular emission lanes”, 2015, Astron. & Astrophys., v578, a135, p1-12.

Wang, K., Testi, L., Ginsburg, A., Walmsley, C.M., Molinari, S., Schisano, E., “Large scale filaments associated with Milky Way spiral arms”, 2015, MNRAS, v450, p4043-4049.

Wu, Y.W., Sato, M., Reid, M.J., Moscadelli, L., Zhang, B., Xu, Y., Brunthaler, A., Menten, K.M., Dame, T.M., Zheng, X.W., “Trigonometric parallaxes of star forming regions in the Sagittarius spiral arm”, 2014, A&A, v566, a17, p1-26.

Zucker, C., Battersby, C., Goodman, A., “The skeleton of the Milky Way”, 2015, ApJ, v815, a23, p1-25.

Table 3 - Catalog of statistical means of arm tangent longitudes for each tracer, in each spiral arm^(a)

Arm Name	Chemical tracer	Tangent ^(b) galactic longitude	Ang. dist. ^(c) to ¹² CO from ¹² CO	Linear separation inside arm ^(cd)	References
Carina	¹² CO at 8'	281.3°	0°	0 pc, at 5 kpc	mean in Table 5
	HI atom	282.1°	0.8°	22 pc	mean in Table 8
	Thermal electron	283°	1.7°	148 pc	Taylor & Cordes (1993 – fig.4)
	HII complex	283.8°	2.5°	218 pc	mean in Table 6
	Dust 240μm	284°	2.7°	235 pc	Drimmel (2000 –fig.1)
	Dust 870 μm	284.2°	2.9°	253 pc	mean in Table 9
	1.4GHz RRL	284.3°	3°	262 pc	Hou & Han (2015 – table 1)
	Dust 60μm	285°	3.7°	322 pc	Bloemen et al (1990 – fig.5)
	FIR [CII] & [NII]	287°	5.7°	497 pc	Steiman-Cameron et al (2010 – sect. 2.1)
Crux-Centaurus	Old stars (1-8 μm)	307.3°	- 2.2°	-230 pc	mean in Table 10
	Thermal electron	309°	- 0.5°	-52 pc	Taylor & Cordes (1993 – fig.4)
	FIR [CII] & [NII]	309°	- 0.5°	-52 pc	Steiman-Cameron et al (2010 – sect. 2.1)
	NH ₃ 1-1 2' cores	309.1°	- 0.4°	-42 pc	Hou & Han (2015 – table 1)
	¹² CO at 8'	309.5°	0°	0 pc, at 6 kpc	mean in Table 5
	HI atom	309.9°	0.4°	42 pc	mean in Table 8
	HII complex	309.9°	0.4°	42 pc	mean in Table 6
	²⁶ Al	310°	0.5°	52 pc	Chen et al (1996- fig.1)
	Sync. 408 MHz	310°	0.5°	52 pc	Beuermann et al (1985 – fig.1)
	Dust 240μm	311°	1.5°	157 pc	Drimmel (2000 – fig. 1)
	Dust 60μm	311°	1.5°	157 pc	Bloemen et al (1990 – fig.5)
	1.4GHz RRL	311.2°	1.7°	178 pc	Hou & Han (2015 – table 1)
	Dust 870μm	311.4°	1.9°	198 pc	mean in Table 9
Norma	²⁶ Al	325°	- 3.4°	-415 pc	Chen et al (1996 – fig.1)
	HII complex	326.4°	- 2.0°	-244 pc	mean in Table 6
	NH ₃ 1-1 2' cores	327.8°	- 0.6°	-73 pc	Hou & Han (2015 – table 1)
	Thermal electron	328°	- 0.4°	-49 pc	Taylor & Cordes (1993 – fig.4)
	Sync. 408 MHz	328°	- 0.4°	-49 pc	Beuermann et al (1985 – fig.1)
	[CII]	328°	- 0.4°	-49 pc	Velusamy et al (2015 – fig.7b)
	HI atom	328.1°	- 0.3°	-37 pc	mean in Table 8
	¹² CO at 8'	328.4°	0°	0 pc, at 7 kpc	mean in Table 5
	Dust 60μm	329°	0.6°	73 pc	Bloemen et al (1990 – fig.5)
	1.4GHz RRL	329.3°	0.9°	110 pc	Hou & Han (2015 – table 1)
	Dust 870μm	329.6°	1.2°	147 pc	mean in Table 9
	Masers	330.4°	2.0°	244 pc	mean in Table 7
	Dust 240μm	332°	3.6°	440 pc	Drimmel (2000 – fig. 1)
	Dust 2.4μm	332°	3.6°	449 pc	Hayakawa et al (1981 – fig.2a)
Start of Perseus	¹² CO at 8'	336.8°	0°	0 pc, at 8 kpc	mean in Table 5
	HI atom	336.8°	0°	0 pc	mean in Table 8
	1.4GHz RRL	336.9°	0.1°	14 pc	Hou & Han (2015 – table 1)
	[CII]	337°	0.2°	28 pc	Velusamy et al (2015 – fig.8b)
	HII complex	337.2°	0.4°	56 pc	mean in Table 6
	Dust 870μm	337.8°	1.0°	140 pc	mean in Table 9
	Masers	337.8°	1.0°	140 pc	mean in Table 7
	FIR [CII] & [NII]	338°	1.2°	167 pc	Steiman-Cameron et al (2010 – sect. 2.1)
	Old stars (1-8 μm)	338.3°	1.5°	209 pc	mean in Table 10

	NH ₃ 1-1 2' cores	338.4 ^o	1.6 ^o	223 pc	Hou & Han (2015 – table 1)
	Sync. 408 MHz	339 ^o	2.2 ^o	307 pc	Beuermann et al (1985 – fig.1)
	Dust 2.4μm	339 ^o	2.2 ^o	307 pc	Hayakawa et al (1981 – fig.2a)
	Dust 60μm	340 ^o	3.2 ^o	446 pc	Bloemen et al (1990 – fig.5)
Start of Sagittarius	¹² CO at 8'	344 ^o	0 ^o	0 pc, at 7.5 kpc	mean in Table 5
	²⁶ Al	346 ^o	2 ^o	262 pc	Kretschmer et al (2013 – fig.9a)
	Masers	346.5	2.5 ^o	327 pc	mean in Table 7
	NIR star counts	348 ^o	4 ^o	520 pc	mean in Table 10
	Dust 870 μm	343 ^o	-1 ^o	-131 pc	mean in table 9
Start of Norma	¹² CO at 8'	020 ^o	0 ^o	0 pc, at 6.5 kpc	Vallée (2016 –Fig.2)
	NIR star counts	019 ^o	1 ^o	113 pc	mean in Table 10
	Sync. 6 GHz	016 ^o	4 ^o	454 pc	Hayakawa et al (1981 – fig. 2b)
	Masers	016.0	4 ^o	454 pc	mean in Table 7
Scutum	¹² CO at 8'	032.9 ^o	0 ^o	0 pc, at 5 kpc	mean in Table 5
	²⁶ Al	032 ^o	0.9 ^o	78 pc	Chen et al (1996 – fig.1)
	Thermal electron	032 ^o	0.9 ^o	78 pc	Taylor & Cordes (1993 – fig.4)
	Sync. 408 MHz	032 ^o	0.9 ^o	78 pc	Beuermann et al (1985 – fig.1)
	Old stars (1-8 μm)	031.3 ^o	1.6 ^o	140 pc	mean in Table 10
	¹³ CO	031.3 ^o	1.6 ^o	140 pc	mean in Table 4
	HI atom	031.0 ^o	1.9 ^o	166 pc	mean in Table 8
	Dust 240μm	031 ^o	1.9 ^o	166 pc	Drimmell (2000 – fig. 1)
	Dust 870μm	030.9 ^o	2.0 ^o	174 pc	mean in Table 9
	1.4GHz RRL	030.8 ^o	2.1 ^o	183 pc	Hou & Han (2015 – table 1)
	Warm ¹² CO cores	030 ^o	2.9 ^o	253 pc	Solomon et al (1985 – fig. 1b)
	FIR [CII] & [NII]	030 ^o	2.9 ^o	253 pc	Steiman-Cameron et al (2010 – sect 2.1)
	HII complex	029.6 ^o	3.3 ^o	288 pc	mean in Table 6
	Dust 2.4μm	029 ^o	3.9 ^o	340 pc	Hayakawa et al (1981 – fig. 2a)
	Masers	028.5 ^o	4.4 ^o	384 pc	mean in Table 7
	Dust 60μm	026 ^o	6.9 ^o	602 pc	Bloemen et al (1990 – fig.5)
	Sagittarius	Old stars (1-8 μm)	055.0 ^o	-4.5 ^o	-314 pc
HII complex		050.6 ^o	-0.1 ^o	-7 pc	mean in Table 6
HI atom		050.6 ^o	-0.1 ^o	-7 pc	mean in Table 8
¹² CO at 8'		050.5 ^o	0 ^o	0 pc, at 4 kpc	mean in Table 5
¹³ CO		050.2 ^o	0.3 ^o	21 pc	mean in Table 4
Dust 240μm		050 ^o	0.5 ^o	35 pc	Drimmell (2000 – fig. 1)
Masers		050.0 ^o	0.5 ^o	35 pc	mean in Table 7
FIR [CII] & [NII]		050 ^o	0.5 ^o	35 pc	Steiman-Cameron et al (2010 – sect. 2.1)
1.4GHz RRL		049.2 ^o	1.3 ^o	91 pc	Hou & Han (2015 – table 1)
Dust 870μm		049.1 ^o	1.4 ^o	98 pc	mean in Table 9
Warm ¹² CO cores		049 ^o	1.5 ^o	105 pc	Solomon et al (1985 – fig. 1b)
Thermal electron		049 ^o	1.5 ^o	105 pc	Taylor & Cordes (1993 – fig.4)
Sync. 408 MHz		048 ^o	2.5 ^o	175 pc	Beuermann et al (1985 – fig. 1)
²⁶ Al		046 ^o	4.5 ^o	316 pc	Chen et al (1996 – fig.1)

Notes: (a): Published since 1980. Updating the earlier table 1 of Vallée (2014b).
(b): When there are 2 or more published reports for a given arm tracer in a given spiral arm, then a separate table is provided (Tables 3 to 10 here).
(c): Angular distance from the arm center, being positive towards the arm's inner edge (towards the Galactic Center), and negative in other direction (towards the galactic anti-center).
(d): Linear separation from the arm center (¹²CO), after converting the angular separation at the arm distance from the sun; using 8.0 kpc for the distance of the Sun to the Galactic Center.

Table 4 - Individually observed tangent longitude for the $^{13}\text{CO J=1-0}$ tracer^(a)

Arm name	Tangent galactic longitude	Telescope HPBW	Survey name	Reference
Scutum	030.5° 032°	46'' 3'	Galactic Ring Bell Labs	Hou & Han (2015- table 1) – reassessed ^(b) Stark & Lee (2006 – fig.1, v= +95 km/s)
031.3° ±1.1°		mean and r.m.s.		
Sagittarius	049.4° 051°	46'' 3'	Galactic Ring Bell Labs	Hou & Han (2015- table 1) – reassessed ^(b) Stark & Lee (2006 – fig.1, v= +60 km/s)
050.2° ±1.1°		mean and r.m.s.		

Notes:

(a): Published since 1980.

(b): Hou & Han (2015) reassessed the published $^{13}\text{CO J=1-0}$ data from Jackson et al (2006).

Table 5 - Individually observed tangent longitude for the $^{12}\text{CO J}=1-0$ tracer^(a)

Arm name	Tangent Galactic longitude	Telescope HPBW	Survey name	Reference
Carina	280°	8.8'	Columbia	Alvarez et al (1990 – table 4)
	280°	8.8'	Columbia	Grabelsky et al (1987 – sect. 3.1.2)
	281°	8.8'	Columbia	Grabelsky et al (1988 – fig.4)
	282°	8.8'	Columbia	Bronfman et al (2000b – table 2)
	282.0	8.8'	Columbia	Hou & Han (2015- table 1) – reassessed ^(b)
	283°	8.8'	Columbia	Bronfman et al (2000a – Section 3.4)
	281.3° ±1.2°	mean and r.m.s.		s.d.m of 0.5°, worth 44 pc at 5 kpc
Crux-Cen-Taurus	308°	8.8'	Columbia	Bronfman et al (2000a – sect. 3.4)
	308°	8.8'	Columbia	Bronfman (2008 – sect. 4)
	309°	8.4'	CfA	Dame & Thaddeus (2011 – fig.4)
	309°	8.8'	Columbia	Bronfman et al (2000b – table 2)
	310°	8.8'	Columbia	Alvarez et al (1990 – table 4)
	310°	8.8'	Columbia	Bronfman et al (1988 – fig. 7)
	310°	8.8'	Columbia	Bronfman et al (1989 – sect. 4)
	310°	8.8'	Columbia	García et al (2014 – table 3)
	310°	8.8'	Columbia	Grabelsky et al (1987 – sect. 3.1.2)
	311.0°	8.8'	Columbia	Hou & Han (2015- table 1) – reassessed ^(b)
	309.5° ±1.0°	mean and r.m.s.		s.d.m of 0.3°, worth 32 pc at 6 kpc
Norma	328°	8.8'	Columbia	Alvarez et al (1990 – table 4)
	328°	8.8'	Columbia	Bronfman et al (1988 – fig. 7)
	328°	8.8'	Columbia	Bronfman et al (1989 – sect. 4)
	328°	8.8'	Columbia	Bronfman (1992 – fig.6)
	328°	8.8'	Columbia	Bronfman et al (2000a – sect. 3.4)
	328°	8.8'	Columbia	Bronfman et al (2000b – table 2)
	328°	8.8'	Columbia	Bronfman (2008 - sect. 4)
	328.3	8.8'	Columbia	Hou & Han (2015- table 1) – reassessed ^(b)
	330°	8.8'	Columbia	García et al (2014 – table 3)
330°	8.8'	Columbia	Grabelsky et al (1987 – sect. 3.1.2)	
	328.4° ±0.8°	mean and r.m.s.		s.d.m of 0.3°, worth 37 pc at 7 kpc
Start of Perseus	336°	8.8'	Columbia	Bronfman et al (1989 – sect. 4)
	336°	8.8'	Columbia	Bronfman (2008 – sect. 4)
	336.7	8.8'	Columbia	Hou & Han (2015- table 1) – reassessed ^(b)
	337°	8.8'	Columbia	Alvarez et al (1990 – table 4)

	337°	8.8'	Columbia	Bronfman et al (2000a – sect. 3.4)
	337°	8.8'	Columbia	Bronfman et al (2000b - table 2)
	337°	8.8'	Columbia	Dame & Thaddeus (2008 – sect. 1)
	338°	8.8'	Columbia	García et al (2014 – table 3)
	336.8° ±0.6°		mean and r.m.s.	s.d.m of 0.3°, worth 42 pc at 8 kpc
Start of Sagittarius	344°	8.8'	Columbia	Grabelsky et al (1987 – fig.6)
	344°	mean		
Scutum	030.5°	8.4'	CfA	Hou & Han (2015- table 1) – reassessed ^(b)
	031°	8.4'	CfA	Dame & Thaddeus (2011 – fig.4)
	033°	1.1'	NRAO	Sanders et al (1985 – fig.5b)
	034°	7.5'	Columbia	Dame et al (1986 – fig.9)
	034°	7.5'	Columbia	Cohen et al (1980 – fig.3)
	035°	1.0'	Texas	Chiar et al (1994 – Sect. 3)
	032.9° ±1.8°		mean and r.m.s.	s.d.m of 0.8°, worth 70 pc at 5 kpc
Sagittarius	049.4	8.4'	CfA	Hou & Han (2015- table 1) – reassessed ^(b)
	051°	7.5'	Columbia	Cohen et al (1980 – fig.3)
	051°	7.5'	Columbia	Dame et al (1986 – fig.9)
	050.5° ±0.9°		mean and r.m.s.	s.d.m of 0.5°, worth 36 pc at 4 kpc

Notes:

(a): Published since 1980.

(b): Hou & Han (2015) reassessed the published ¹²CO 1-0 data from Dame et al (2001).

Table 6 – Individually observed tangent longitude for the HII region tracer^(a)

Arm name	Tangent galactic longitude	Range	Reference
Carina	283.3°	radio-IR-opt.	Hou & Han (2015 – table 1) – reassessed ^(a)
	284°	optical	Russeil (2003 – table 6)
	284°	radio	Downes et al (1980 – fig.4)

	283.8° ±0.3°	mean and r.m.s.	
Crux-Centaurus	309°	optical	Russeil (2003 – table 6)
	309°	radio	Downes et al (1980 – fig.4)
	311.7°	radio-IR-opt.	Hou & Han (2015 – table 1) – reassessed ^(a)

	309.9° ±1.6°	mean and r.m.s.	
Norma	323°	optical	Russeil (2003 – table 6)
	328°	radio	Downes et al (1980 – fig.4)
	328.1°	radio-IR-opt.	Hou & Han (2015 – table 1) – reassessed ^(a)

	326.4° ±2.9°	mean and r.m.s.	
Start of Perseus	337.2°	radio-IR-opt.	Hou & Han (2015 – table 1) – reassessed ^(a)

	337.2°	mean	
Scutum	025°	radio	Sanders et al (1985 – fig. 5a)
	030.6°	radio-IR-opt.	Hou & Han (2015 – table 1) – reassessed ^(a)
	031°	radio	Downes et al (1980 – fig.4)
	032°	optical	Russeil (2003 – table 6)

	029.6° ±3.1°	mean and r.m.s.	
Sagittarius	046°	radio	Downes et al (1980 – fig.4)
	049.4°	radio-IR-opt.	Hou & Han (2015 – table 1) – reassessed ^(a)
	051°	optical	Russeil et al (2007 – fig.4)
	056°	optical	Russeil (2003 – table 6)

	050.6° ±4.2°	mean and r.m.s.	

Notes:

(a): Published since 1980.

(b): Hou & Han (2015) reassessed the published HII regions data from Anderson et al (2014).

Table 7 –Individually observed tangent longitude for the maser tracer^(a)

Arm name	Tangent Galactic longitude	Maser name	Reference
Carina	284.5°	methanol	Hou & Han (2015 – table 1) – reassessed ^(b)
	284.5°	mean	
Crux-Centaurus	312.2°	methanol	Hou & Han (2015 – table 1) – reassessed ^(b)
	312.2°	mean	
Norma	329.3°	methanol	Hou & Han (2015 – table 1) – reassessed ^(b)
	331.5°	methanol	Caswell et al (2011 – Sect. 4.6.2)
	330.4° ±1.5°	mean and r.m.s.	
Start of Perseus	337.0°	methanol	Hou & Han (2015 – table 1) – reassessed ^(b)
	338°	methanol	Green et al (2011 – sect. 3.3.1)
	338°	methanol	Green et al (2012 – Sect.2)
	338°	methanol	Caswell et al (2011 – sect. 4.6.1)
	337.8° ±0.5°	mean and r.m.s.	
Start of Sagittarius	344°	H ₂ O & methanol	Sanna et al (2014 – fig. 6)
	349°	methanol	Green et al (2011 – table 1)
	346.5° ±3.5°	mean and r.m.s.	
Start of Norma	020°	methanol	Green et al (2011 – table 1)
	012°	methanol	Green et al (2011 – table 1)
	016.0° ±5.6°	mean and r.m.s.	
Scutum	025°	H ₂ O & methanol	Sanna et al (2014 – fig.6)
	026°	methanol	Green et al (2012 – Sect.2)
	028°	methanol	Green et al (2011 – sect. 3.3.1)
	030°	meth., water	Reid et al (2014 – fig.1)
	030.8°	methanol	Hou & Han (2015 – table 1) – reassessed ^(b)
	031°	meth., water	Sato et al (2014 – fig3)
	028.5° ±2.6°	mean and r.m.s.	
Sagittarius	049.3°	methanol	Hou & Han (2015 – table 1) – reassessed ^(b)

049.6°	methanol	Pandian & Goldsmith (2007 – sect.4)
050°	meth., water	Reid et al (2014 – fig.1)
051°	meth., water	Wu et al (2014 – sect. 4.2)

050.0° ±0.7° mean and r.m.s.

Notes:

(a): Published since 1980

(b): Hou & Han (2015) reassessed the published methanol masers catalog from Hou & Han (2014).

Table 8 - Individually observed tangent longitude for the HI atom tracer^(a)

Arm name	Tangent Galactic Longitude	Telescope HPBW	Survey name	Reference
Carina	281.2°	36'	Leiden	Nakanishi & Sofue (2016- fig.7) ^(b)
	283.0°	36'	LAB	Hou & Han (2015 – Table 1) ^(c)
	282.1° ±1.3°		mean and r.m.s.	
Crux-Centaurus	309.3°	36'	Leiden	Nakanishi & Sofue (2016- fig.7) ^(b)
	310°	15' – 36'	Hat Creek;Parkes	Englmaier & Gerhard (1999- table 1)
	310.4°	36'	LAB	Hou & Han (2015 – Table 1) ^(c)
309.9° ±0.6°		mean and r.m.s.		
Norma	328.0°	36'	LAB	Hou & Han (2015 – Table 1) ^(c)
	328.0°	15' – 36'	Hat Creek;Parkes	Englmaier & Gerhard (1999- table 1)
	328.4°	36'	Leiden	Nakanishi & Sofue (2016- fig.7) ^(b)
328.1° ±0.2°		mean and r.m.s.		
Start of Perseus	336.8°	36'	LAB	Hou & Han (2015 – Table 1) ^(c)
	336.9°	36'	Leiden	Nakanishi & Sofue (2016- fig.7) ^(b)
	336.8° ±0.1°		mean and r.m.s.	
Scutum	029°	15' – 36'	Hat Creek;Parkes	Englmaier & Gerhard (1999 – table 1)
	030.8°	36'	LAB	Hou & Han (2015 – Table 1) ^(c)
	033.2°	36'	Leiden	Nakanishi & Sofue (2016- fig.7) ^(b)
031.0° ±2.1°		mean and r.m.s.		
Sagittarius	050°	15' – 36'	Hat Creek;Parkes	Englmaier & Gerhard (1999 – table 1)
	050.8°	36'	LAB	Hou & Han (2015 – Table 1) ^(c)
	051.0°	36'	Leiden	Nakanishi & Sofue (2016- fig.7) ^(b)
050.6° ±0.5°		mean and r.m.s.		

Notes:

(a): Published since 1980.

(b): Nakanishi & Sofue (2016) reassessed the published HI catalogs from Hartmann & Burton (1997) and Bajaja et al (2005); they added the CO survey of Dame et al (2001).

(c): Hou & Han (2015) reassessed the published HI catalog from Kalberla et al (2005).

Table 9 - Individually observed tangent longitude for the dust 870 μ m trace^(a)

Arm name	Tangent galactic longitude	Teles-cope HPBW	Survey name	Reference
Carina	284.2.0 ^o	19"	Atlasgal	Hou & Han (2015 – Table 1) ^(b)
	284.2 ^o	mean		
Crux-Centaurus	311 ^o	19"	Atlasgal	Beuther et al (2012 – fig.2)
	311.7 ^o	19"	Atlasgal	Hou & Han (2015 – Table 1) ^(b)
	311.4 ^o \pm 0.5 ^o	mean and r.m.s.		
Norma	327.2 ^o	19"	Atlasgal	Hou & Han (2015 – Table 1) ^(b)
	332 ^o	19 "	Atlasgal	Beuther et al (2012 – fig.3)
	329.6 ^o \pm 3.4 ^o	mean and r.m.s.		
Start of Sagittarius	343 ^o	19"	Atlasgal	Beuther et al (2012 – fig.3)
	343 ^o	mean		
Start of Perseus	337.5 ^o	19"	Atlasgal	Hou & Han (2015 – Table 1) ^(b)
	338 ^o	19"	Atlasgal	Beuther et al (2012 – fig.3)
	337.8 ^o \pm 0.3 ^o	mean and r.m.s.		
Scutum	031 ^o	19"	Atlasgal	Beuther et al (2012 – fig.3)
	030.7 ^o	19"	Atlasgal	Hou & Han (2015 – Table 1) ^(b)
	030.9 ^o \pm 0.2 ^o	mean and r.m.s.		
Sagittarius	049.2 ^o	19"	Atlasgal	Hou & Han (2015 – Table 1) ^(b)
	049 ^o	19"	Atlasgal	Beuther et al (2012 – fig.3)
	049.1 ^o \pm 0.2 ^o	mean and r.m.s.		

Notes:

(a): Published since 1980.

(b): Hou & Han (2015) reassessed the published HI catalogs from Contreras et al (2013) and Csengeri et al (2014).

Table 10 - Individually observed tangent longitude for the 1 μ m to 8 μ m old stars tracer ^(a)

Arm name	Tangent galactic longitude	Teles-cope HPBW	Survey name	Reference
Crux-Centaurus	307 $^{\circ}$	21'	COBE K-band 2 μ m	Drimmel (2010 – Sect.3)
	307.5 $^{\circ}$	1.2;2"	GLIMPSE; 2MASS	Hou & Han (2015 – Table 1) ^(b)
	307.3 $^{\circ}$ \pm 0.4 $^{\circ}$	mean and r.m.s.		
Start of Perseus	338.3 $^{\circ}$	1.2";2"	GLIMPSE; 2MASS	Hou & Han (2015 – Table 1) ^(b)
	338.3 $^{\circ}$	mean		
Start of Sagittarius	348 $^{\circ}$	21'	J,H,K COBE	Benjamin (2008 – Fig.2)
	348 $^{\circ}$	mean		
Start of Norma	019 $^{\circ}$	21'	J,H,K COBE	Benjamin (2008 – Fig.2)
	019 $^{\circ}$	1.2;2"	4.5 μ m GLIMPSE	Benjamin (2008 – Fig.2)
	019 $^{\circ}$	mean		
Scutum	030 $^{\circ}$	21'	COBE K-band 2 μ m	Drimmel (2010 – Sect.3)
	032.6 $^{\circ}$	1.2";2"	GLIMPSE; 2MASS	Hou & Han (2015 – Table 1) ^(b)
	031.3 $^{\circ}$ \pm 1.8 $^{\circ}$	mean and r.m.s.		
Sagittarius	055.0 $^{\circ}$	1.2";2"	GLIMPSE; 2MASS	Hou & Han (2015 – Table 1) ^(b)
	055.0 $^{\circ}$	mean		

Notes:

(a): published since 1980.

(b): Hou & Han (2015) reassessed the published old star catalogs from Benjamin et al (2003; GLIMPSE) and Skrutskie et al (2006; 2MASS).